Springer

KSME

Journal of Mechanical Science and Technology 26 (9) (2012) 2751~2758
www.springerlink.com/content/1738-494x
DOI 10.1007/s12206-012-0721-z

A study on the exit flow characteristics determined by the orifice configuration of multi-perforated tubes †

Sangkyoo Lee[1], Namsoo Moon[2] and Jeekeun Lee[3,*]

[1]*Department of Precision Mechanical Engineering, Chonbuk National University, Jeonju, Jeonbuk 561-756, Korea*
[2]*Jeonbuk Institute of Automotive Technology, Gunsan-si, Jeonbuk 565-902, Korea*
[3]*School of Mechanical System Engineering, Chonbuk National University, Jeonju, Jeonbuk 561-756, Korea*

(Manuscript Received January 19, 2011; Revised January 1, 2012; Accepted April 4, 2012)

Abstract

A multi-perforated tube indicates the existence of multiple holes in various shapes on the surface of long cylinder-type or rectangular tubes, and the hole installed on the surface is called an orifice as it is relatively small in size, compared with the surface area of the tubes. In this study, flowrate distribution features and changes in discharge angle according to the blockage ratio resulting from the changes in the number of orifices and the thickness of multi-perforated tubes were investigated by means of analysis and experiment, targeting the multi-perforated tubes where rectangular orifices are installed on the both sides of square tubes. In addition, contraction coefficient and flow coefficient between orifices were analytically investigated. The more increase in blockage ratio of multi-perforated tubes, the more uniform flowrate distribution between orifices. The discharge angle becomes more and more perpendicular in the longitudinal direction of multi-perforated tubes as it gets closer to the end of orifices, exhibiting big differences at the entrance if blockage ratio is small. The more increase in the thickness of multi-perforated tubes, the more uniform flowrate distribution between orifices become as contraction coefficient increases. The flow coefficient distribution of orifices using the pressure at the entrance of the orifices of multi-perforated tubes increases in the longitudinal direction of the multi-perforated tubes, exhibiting values ranging from 0.66 to 0.68 as to BR = 0.893 ~ 0.979.

Keywords: Multi-perforated tube; Blockage ratio; Orifice flow; Flow distribution; Flow coefficient

1. Introduction

A multi-perforated tube means the existence of multiple holes in various shapes on the surface of long cylinder-type or rectangular tubes, and the hole installed on the surface is called an orifice as it is relatively small in size, compared with the surface area of the tubes. The multi-perforated tubes are widely being used throughout the entire industry as they can play the role of a flow divider capable of ejecting flow by dividing it as many as the number of orifices installed on the surface [1-16]. However, because of the features of multi-perforated tubes of a long length, the flow between orifices is not even due to change in pressure in the longitudinal direction, and the discharge angle of the stream released from orifices is known to be different from each location [4-7]. Therefore, a number of studies have been conducted for the purpose of obtaining mathematical formulae capable of controlling and predicting the flow and discharge angle between the orifices installed in the longitudinal direction of multi-perforated tubes.

Ahn [1] fixed the diameter of orifices in a one-dimensional channel flow in the low Reynolds numbers, and studied flowrate distribution characteristics as per the variables non-dimensionalized by the size of inlets and outlets, and the Reynolds numbers by means of analysis and experiment. Foust [2] investigated the velocity and the flow structures of multiple jets emitted after being passed through multi-perforated tubes with various diameters and pitches of orifices using PIV for Catheter-an intravascular syringe needle in medicine. Chen [3, 4] performed an analytical and experimental research on the characteristics of flowrate distribution using multi-perforated tubes where rectangular orifices were installed. He discovered that the flowrate change between each orifice was very small at sufficiently fast speed inside tubes, verifying the discharge angle of stream gets closer to 90° in the longitudinal direction as it moves to the end of tubes. He also analytically investigated that the flowrate distribution between orifices could be controlled by changing aspect ratio of orifices. Moueddeb [5, 6] represented the flowrate distribution characteristics in multi-perforated tubes with orifices in various shapes as a one-dimensional equation using the internal static pressure. In

*Corresponding author. Tel.: +82 63 270 2369, Fax.: +82 63 270 2388
E-mail address: leejk@jbnu.ac.kr
† Recommended by Associate Editor Yang Na

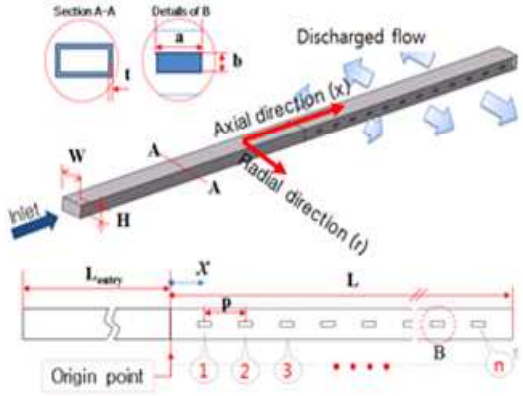

Fig. 1. Schematics of multi-perforated tube and definitions of geometric parameter.

addition, using a manometer, the discharge angle of the flow passing through orifices was measured, and using C_d and C_r (regain coefficient), a mathematical formula close to actual flow was induced, and then, through an experimental verification, the validity of the mathematical formula was confirmed within 10.3% of error range. Singh [7] induced a simple one-dimensional theoretical formula designing the pitch and size of orifices of multi-perforated tubes used for the systems for preventing hazardous materials and for solving safety-related problems in nuclear power plants.

Such studies have been carried out with respect to the flowrate distribution of multi-perforated tubes where the intervals between orifices were not considered, targeting multi-perforated tubes where a single orifice is installed [8-17]. The studies on the multi-perforated tubes with orifices arrayed in more than two rows are rare, and such studies have been mainly limited to the low Reynolds numbers.

For such a reason, this study investigated the influence over the flowrate distribution features and changes in discharge angle between orifices using the changes in the intervals between orifices and blockage ratio (BR) via the changes in the number of orifice, targeting multi-perforated tubes where rectangular orifices are installed on the both sides of square tubes in relatively high Reynolds numbers. Also, the influence of thickness of orifices was investigated, and, ultimately, design variables affecting the flowrate distribution between orifices were pursued.

2. Analysis methods

2.1 Shape of multi-perforated tubes

The shape of the multi-perforated tubes used for the analysis and experiment is as follows, as shown in Fig. 1.

The multi-perforated tubes were designed as a 2-dimensional model, and, in order to create a fully-developed flow field, an entrance length equivalent to the fiftyfold diameter of the entrance of multi-perforated tubes was installed. The point where the entrance length ends was set as the starting point, and the longitudinal direction of the multi-perforated tubes was set as an axial direction (flow direction, x-dir), and the direction perpendicular to the axial direction as a radial direction (r-dir). The end of the multi-perforated tube is blocked and the interval between the starting point and the first orifice and the distance from the end to the last orifice are the same.

Table 1. Analysis conditions. (unit: mm)

Case	BR	NO of orifice	Pitch	t	W	H	L	a	b
1	0.979	8	57.78	2 or 10	50	25	600	10	4
2	0.968	12	36.92						
3	0.957	16	25.88						
4	0.946	20	19.05						
5	0.936	24	14.40						
6	0.893	40	4.87						

Table 2. Inlet boundary conditions.

	Re ($\times 10^4$)	m_{water} (kg/s)	Q_{water} x10^{-3}(m^3/s)	Inlet velocity (m/s)
1	5	0.380	0.381	0.305
2	7	0.532	0.534	0.427
3	10	0.760	0.762	0.610
4	20	1.521	1.524	1.220
5	40	3.042	3.049	2.439

As for the multi-perforated tubes, the rectangular orifices with an aspect ratio of 0.4 were installed on the both sides of square tubes with an aspect ratio of 0.5. The aspect ratios of orifices were the same, and blockage ratio was adjusted by changing the number of orifices. The blockage ratio here can be defined as a value divided the difference between the area of the both sides of a square tube where orifices are installed and the area of an orifice by the area of the both sides of a square tube where orifices are installed. Now that the starting point and ending point of the orifices were fixed, the pitches between the orifices were automatically adjusted according to the changes in the number of the orifices. The number of orifices had been changed from 9 to 40, and the changes in the pitch between orifices and the blockage ratio thereby were shown in Table 1. As for the number of orifices, the orifice closest to the starting point is defined as number 1, and the locations of orifices are displayed after their being non-dimensionalized using L-the length from the starting point to the end of the orifices.

2.2 Analysis conditions

The analysis for investigating the flowrate distribution features and changes in discharge angle of the stream between the orifices of multi-perforated tubes was performed in accordance with the changes in the Reynolds numbers, as shown in Table 2, with respect to the geometrical conditions shown in

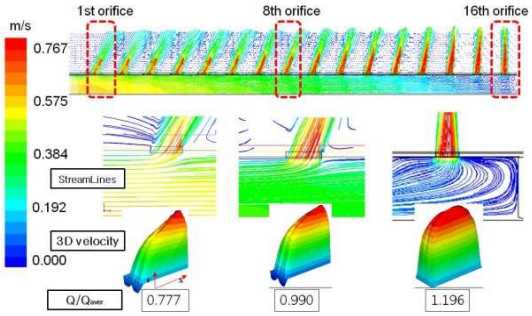

Fig. 2. Velocity vector plots and streamlines around orifice exit.

Fig. 3. Photo of orifice arrange along the tube and discharged flow through orifices.

Table 1. At this point, the experimental verification of the analysis results was performed at Re = $7x10^4$. The analytical research was performed using a commercial software, Fluent V.6.3, widely being used in the area of flow analysis. The turbulence model applied to the analysis was the k-ε real model [3, 4], which is known to be able to perform relatively accurate calculation in the event of big changes in curvatures of streamlines, at the same time being suitable for rotation and the flow field of recirculation. The water density, a working fluid, of 998 kg/m^3 at 20℃, and a viscosity coefficient of $1.005x10^{-3}$ kg/m. s, were applied. The entrance pressure of an orifice is set as atmospheric pressure, and the flowrate distribution passing through the orifice was allowed to be observed by setting a flow area at the entrance of the orifice.

3. Results and discussion

3.1 Internal or external flow characteristics of multi-perforated tubes

Fig. 2 indicates the streamlines of internal and external flow fields of multi-perforated tubes when BR = 0.957 and Re = $7x10^4$, and velocity is expressed in colors. The internal flow inside multi-perforated tubes produced big changes, affected by the orifices installed in the longitudinal direction of the tubes, displaying drastic changes in the streamlines near the entrance of the orifices. Also, highly complicated flow characteristics are shown at the end of the tubes including recirculation areas. Such complicated internal flow characteristics are resulted from the changes in velocity, momentum, pressure, etc. as a consequence of the emission coming through orifices as fluid runs in the direction of the longitudinal direction of tubes.

The flow field at the exit of orifices, formed outside the multi-perforated tubes, is directly affected by the internal flow characteristics. The velocity distribution between orifices becomes more uniform as it moves closer to the end of tubes; consequently, it can be seen that the amount of flowrate is bigger at the end of tubes than at the entrance. The discharge angle passing through orifices becomes more and more perpendicular to the surface of the entrance as it gets closer to the end of multi-perforated tubes.

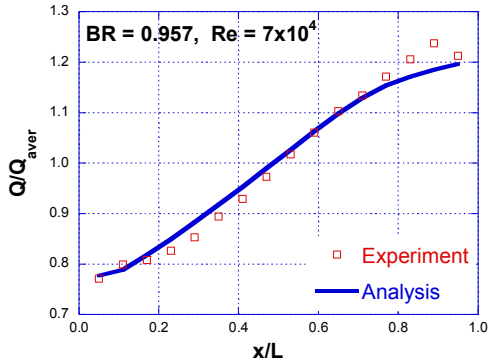

Fig. 4. Volume flowrate distributions with axial distance.

Based on such results, it can be said that the internal and external flow characteristics of multi-perforated tubes are affected by the geometrical variables as the number of orifices (that is, the blockage ratio), which affects change in pressure inside the tubes or the intervals between orifices, etc., and the characteristics of such variables should be expressed as functions in the longitudinal direction of multi-perforated tubes.

Fig. 3 is an image of the working fluid stream passing through orifices when BR = 0.957 and Re = $7x10^4$, which is the same condition as the analysis result shown in Fig. 2. Compared with the analysis result shown in Fig. 2, it can be seen that the macroscopic features including flow direction look similar. For a quantitative investigation, the discharged flowrate between orifices was measured and compared with the analysis result. The measurement of the discharged flowrate was carried out over the period of time sufficiently long enough to ignore time variation effects, and the experimental errors were minimized by iterating the experiment.

Fig. 4 is a comparison of the measurement results of the discharged flowrate between orifices obtained from the same condition, as shown in Fig. 3, with the analysis results. Tough the analysis results were slightly high at the entrance of multi-perforated tubes and slightly low at the end, it can be seen that they are relatively consistent in the entire longitudinal direction. The standard deviation of the analysis result with respect to the experimental values in the entire longitudinal direction of the multi-perforated tubes was 0.0224, which is a reasonable value for investigating the flow characteristics of multi-perforated tubes.

3.2 Characteristics of flowrate distribution between orifices of multi-perforated tubes

Fig. 5 illustrates the flowrate distribution between orifices when BR has been changed from 0.893 to 0.978 at Re = $7x10^4$.

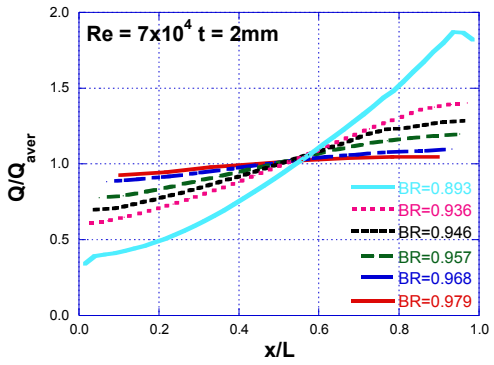

Fig. 5. Volume flowrate distribution along the tube with BR in Re = $7x10^4$.

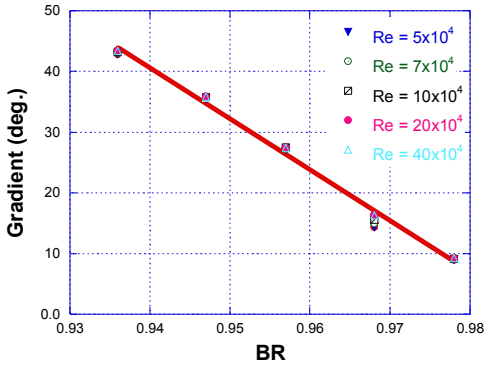

Fig. 6. Gradient of flowrate distribution with the Reynolds number.

Even if the orifices area installed discontinuously, they are expressed in a continuous manner in order to understand the flowrate distribution features in the longitudinal direction of multi-perforated tubes. The x/L = 0 on the graph represents the entrance of a multi-perforated tube, and x/L = 1 its end. The flowrate distribution between orifices in the longitudinal direction of multi-perforated tubes exhibits a relatively linear distribution, showing the biggest difference in flowrate distribution between the entrance of tubes and the end when big discharging areas resulting from the large number of installation of orifices of BR = 0.893. It can be seen that the flowrate distribution between orifices in the longitudinal direction of tubes becomes more and more uniform because a decrease in the number of installed orifices leads to the decrease in size of the discharging area.

Fig. 6 displays the linear slope values of the flowrate distribution between orifices in the longitudinal direction of multi-perforated tubes shown in Fig. 5 according to the changes in BR as to the various changes in the Reynolds numbers. The Reynolds number had changed within the range of $5\sim40x10^4$, and $20\sim40x10^4$ are relatively high Reynolds numbers. The slope of flowrate distribution between orifices resulting from changes in the Reynolds number does not exhibit big differences with respect to the equivalent BR, showing a similar tendency over the entire BR that had been investigated. When it comes to changes in BR, the more increase in BR, in other

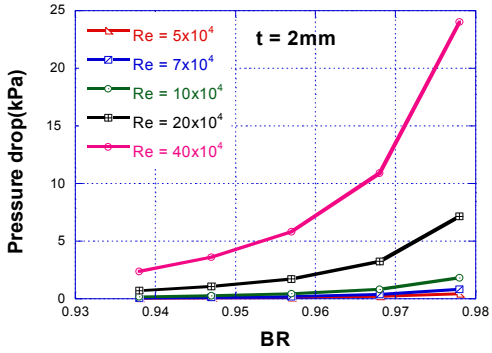

Fig. 7. Static pressure distribution with the Reynolds number.

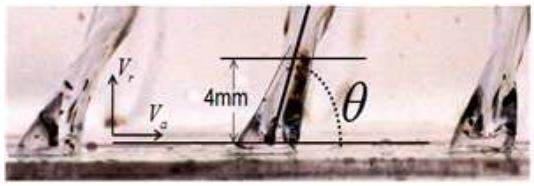

Fig. 8. Photo of water jet structure and definition of discharged angle (θ).

words, the more discharging area decreases as a result of the decrease in the number of orifices, the more slope decreases almost linearly in the investigated Reynolds numbers. Such results mean a growing uniformity of flowrate distribution between orifices as a consequence of a decrease in discharging area of multi-perforated tubes, while being able to be expressed by the following equation:

$$\text{Gradient(deg)} = -839.45\text{BR} + 829.74\,. \quad (1)$$

Fig. 7 displays the changes in the static pressure at the entrance of multi-perforated tubes according to BR with respect to multiple Reynolds numbers. As the BR increases, the pressure tends to increase as expected, especially showing a drastic increase after BR = 0.97.

3.3 Changes in discharge angle between orifices

Fig. 8 is a magnified image of around orifices for measuring the discharge angle of the stream that changes in the longitudinal direction of multi-perforated tubes, as shown in Figs. 2 and 3. It can be seen that the stream discharged from the orifices is being spread after creating a minimum area as it fails to have a structure of the same shape as orifice, becoming more and more contracted by inertia. The point where the minimum sectional area is formed may vary between orifices, but, on average, it exists near the point of 4 mm. The discharge angle was defined as an angle between the line connecting the minimal sectional area where geometrical center and contraction phenomenon occur at the entrance of orifices and the axial direction (x-dir).

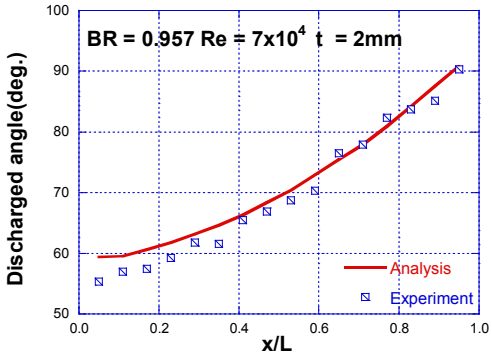

Fig. 9. discharge angle at BR = 0.957, Re = $7x10^4$.

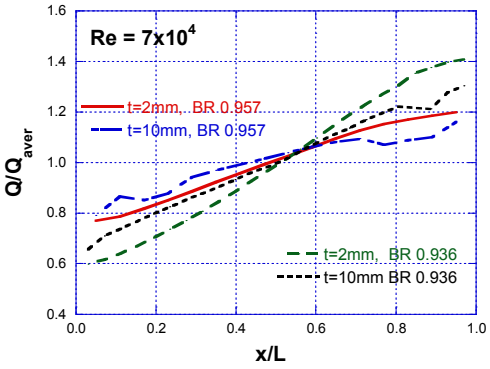

Fig. 11. Flow gradient of a compare with thickness.

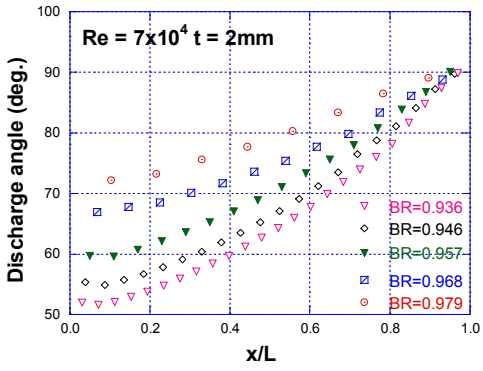

Fig. 10. Discharge angle with BR in Re = $7x10^4$.

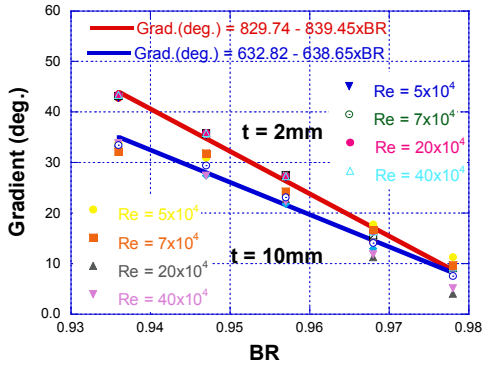

Fig. 12. Gradient of volume flowrate distribution with tube thickness.

Furthermore, a calculation of discharge angle using the analysis results was performed using the size of the velocity component (V_a) in the axial direction and velocity component (V_r) in the radial direction of the calculation point, and then expressed by the average value of the entire sectional area of the entrance, which can be expressed by the formula shown in Eq. (2).

$$\theta(\text{deg}) = \frac{\sum_{i=1}^{n} \tan^{-1}\left(\frac{V_r}{V_a}\right)}{n}, (V_r > 0) \quad (2)$$

Fig. 9 is a comparison of the discharge angle obtained from the experiment when BR = 0.957 and Re = $7x10^4$ with the analysis results. The analysis results exhibit a slightly low discharge angle at the entrance of multi-perforated tubes, showing a tendency in agreement with experimental results, with it getting closer to the end via the center of multi-perforated tubes. The standard deviation of the analysis results as to the experimental values in the entire longitudinal direction of multi-perforated tubes is 1.55. Such a result corresponds to 7.7% of the difference in discharge angle between the inlet and outlet of multi-perforated tubes, which is approximately 20°, and the discharge angle in the stream was investigated using the analysis results within such an error range.

Fig. 10 indicates changes in the discharge angle of a stream passing orifices at Re = $7x10^4$ with respect to the BR in the longitudinal direction of multi-perforated tubes.

The changes in the discharge angles, resulting from a BR, is the biggest at the entrance of multi-perforated tubes, exhibiting a difference of maximum 20° between 0.98 where the BR is the biggest and 0.936 where the BR is the smallest. The changes in discharge angle in the longitudinal direction of multi-perforated tubes indicate low discharge angles at the entrance, and the closer the end is, the closer the angle to 90°. The difference between the entrance where the BR is the smallest (0.936) and the end is about 40°. Also, the changes in discharge angle in the longitudinal direction of multi-perforated tubes tend to be almost linear as BR increases.

3.4 Effect of the thickness of multi-perforated tubes

Fig. 11 illustrates the effect of the thickness of multi-perforated tubes on the flowrate distribution characteristics between orifices. Generally, the thickness of commercial-purpose tubes used for manufacturing multi-perforated tubes ranges from minimum 2 mm to maximum 15 mm [18]. This study investigated the effect of thickness of multi-perforated tubes after selecting thickness of 2 mm and of 10 mm. The BRs applied here were 0.957 and 0.938, and the Reynolds number was $7x10^4$. The changes in thickness of multi-perforated tubes shall lead to an increase in the length of orifices, affecting the flow loss and flow direction of the stream

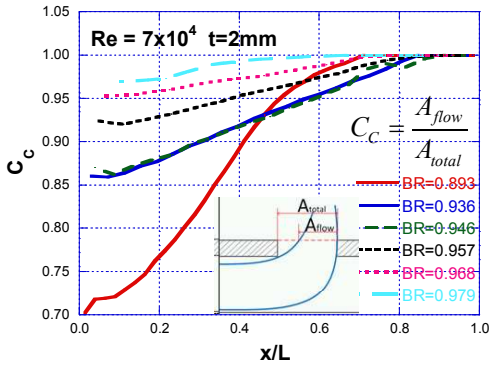

Fig. 13. Contraction coefficient along axial distance for two tube thickness at BR = 0.975, Re = 7x10^4.

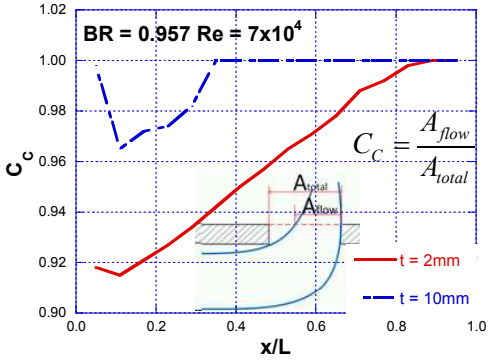

Fig. 14. Contraction coefficient along axial distance with various BR at Re = 7x10^4.

passing through orifices. A multi-perforated tube of thickness of 10 mm results in a higher flowrate distribution at the entrance of the tube than the case of 2 mm, consequently exhibiting a tendency of more uniform flowrate distribution between orifices.

Fig. 12 shows the changes in the slope of flowrate distribution between orifices when t = 2 mm, along with the case when t = 10 mm. When t = 10 mm, the slope of flowrate distribution between orifices according to the changes in the Reynolds numbers shows a similar result as to the same BR as in the case of t = 2 mm. Also, it can be seen that the slope within the range of the investigated Reynolds numbers decreases almost linearly as the BR increases. However, when t = 10 mm, the slope is smaller, showing a small value at a degree of about 10° at BR = 0.936. Such results allow to predict the fact that the more increase in thickness of multi-perforated tubes shall lead to changes in an overall discharge flowrate by affecting the flow coefficients of orifices.

3.5 Distribution of flow coefficient

Fig. 13 shows the changes in contraction coefficient as per the BR at t = 2 mm and Re = 7x10^4 in the longitudinal direction of multi-perforated tubes. The contraction coefficient here was defined as a ratio of geometrical sectional area of an orifice to actual discharge area, and the actual discharge area was defined as an area representing the positive (+) velocity in the radial direction at the calculation point. The changes in contraction coefficient in the longitudinal direction of multi-perforated tubes indicate low values along with the big changes at the entrance of multi-perforated tubes, and the closer to the end, the closer to 1. The smaller a BR is, that is, if a discharge area is relatively big due to a large number of orifices, the lower contraction coefficient distribution gets. In particular, in case of the smallest BR (0.893), about 70% of discharging area at the entrance of tubes is shown. It can be seen that such a change in contraction coefficient is one of the reasons that result in changes in flowrate distribution and discharge angle between orifices, as shown in Figs. 5 and 10.

Fig. 14 illustrates the distribution of contraction coefficient

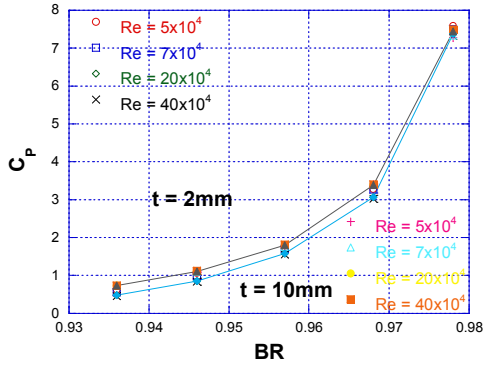

Fig. 15. Pressure coefficient with BR for two tube thickness.

in the longitudinal direction of multi-perforated tubes when BR = 0.957 and Re = 7x10^4 with respect to the case of 2 mm and 10 mm. When the thickness of a multi-perforated tube is 10 mm, changes occur at the entrance of the tube along with low contraction coefficient, but 1 is maintained after x/L = 0.35. On the other hand, in case of 2 mm, a low value less than 1 is shown in the overall longitudinal direction of the tube. Such a result is in agreement with the relatively uniform tendency when thickness increases in the flowrate distribution between orifices, as shown in Figs. 11 and 12.

Fig. 15 indicates the pressure coefficient as to the changes in the BR when t = 2 mm and 10 mm as to the changes in the Reynolds numbers. The definition of pressure coefficient can be expressed by Eq. (3), and POP and mean pressure at the starting point and velocity, respectively.

$$C_P = \frac{P_{static}}{P_{dynamic}} = \frac{P_{OP} - P_{atm}}{\frac{1}{2}\rho V^2} \quad (3)$$

It can be seen that the more increase in BR tends to lead to the more increase in pressure coefficient, exhibiting a pattern similar to the static pressure distribution, as shown in Fig. 7. As for the influence caused by thickness, the case of t = 10 mm yields a relatively low pressure coefficient. It is assumed that such a result means that the increase in discharge area

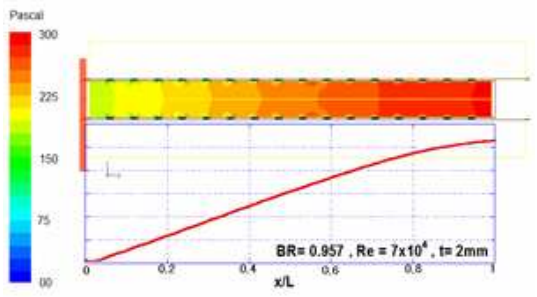

Fig. 16. Static pressure distribution along the centerline of duct.

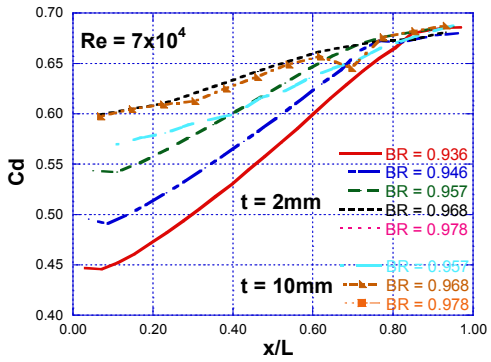

Fig. 17. Discharged coefficient along the axial distance with BR for the thickness of two tubes.

verified in Fig. 14 may have lowered internal static pressure, while decreasing pressure coefficient.

Fig. 16 displays iso-pressure contours inside a multi-perforated tube and the static pressure distribution on the center line. The closer to the end of a multi-perforated tube, the more increase in static pressure, and a big pressure change is shown as a result of the loss of momentum due to the leakage of working fluid between orifices. The reason that the internal pressure of a tube is not uniform, changing in the longitudinal direction, can be understood that the blockage at the end of the tube converts dynamic pressure into static pressure as working fluid moves closer to the end of the tube. Such an ununiform internal pressure distribution has a huge impact on the flowrate distribution between orifices, and, ultimately, can be quantified as a flow coefficient of orifices.

Fig. 17 indicates a flow coefficient according to the change in BR when Re = $7x10^4$ as to t = 2mm and 10 mm. For the calculation of the flow coefficient, Eq. (4) was used.

$$C_d = \frac{m}{A\sqrt{2\rho\Delta P}} \quad (4)$$

The pressure used here is the pressure at the meeting point of the center lines of the multi-perforated tube and orifice, as shown in Fig. 16. Therefore, the flow coefficient means a value for each orifice. The flow coefficient exhibits a low value at the entrance of multi-perforated tubes, as shown in the contraction coefficient in Fig. 13 and the flowrate distribution characteristics between orifices, as shown in Fig. 5, converging to a certain value as it gets closer to the end, especially showing big differences as per the changes in the BR at the entrance, and, generally, exhibiting a high Cd value when t = 10 mm. The C_d value at the end of the orifice ranges from 0.66 to 0.68, and such a result is akin to 0.65 suggested by Moueddeb [5, 6] et al.

4. Conclusion

Targeting multi-perforated tubes where rectangular orifices are installed on the both sides of square tubes, the flowrate distribution characteristics and influence on changes in discharge angle between orifices were investigated using blockage ratio (BR) and changes in thickness as per the changes in the number of orifices. From an analytical and experimental research, the following conclusions were obtained.

(1) The more increase in BR of multi-perforated tubes, the more uniform flowrate distribution between orifices, and it was understood that the linear slope of flowrate distribution in the longitudinal direction of multi-perforated tubes between BR = 0.893~0.979 can be expressed as Grad. (deg) = -839.45BR + 829.74.

(2) The discharge angle between orifices of multi-perforated tubes becomes perpendicular in the longitudinal direction of multi-perforated tubes as it gets closer to the end of orifices, and it was verified that big differences were shown at the entrance if BR was small.

(3) The more increase in the thickness of multi-perforated tubes, the more the flowrate distribution between orifices tends to be uniform, at the same time exhibiting an increase in the contraction coefficient of orifices.

(4) The flow coefficient distribution of orifices using the pressure at the entrance of the orifices of multi-perforated tubes increase in the longitudinal direction, exhibiting values ranging from 0.66 to 0.68 at the end as to BR = 0.893~0.979.

Purpose of this paper is to obtain uniform flowrate distribution, Re, BR, and with a change of T was able to get uniform flowrate distribution. Studies conducted in the range of optimal flowrate distribution gradient, Re = $20x10^4$, T = 10 mm and BR = 0.979 when it was.

Nomenclature

BR	: Blockage ratio
AR	: Aspect ratio
Re	: Reynolds number
V_r	: Radial velocity (m/s)
V_a	: Axial velocity (m/s)
CP	: Pressure coefficient
Q_{aver}	: Averaged volume flowrate through all orifices

References

[1] H. B. Ahn, S. H. Lee and S. H. Shin, Flow distribution in

Manifolds for Low Reynolds Number Flow, *KSME International Journal,* 12 (1997) 87-95.

[2] J. Foust and D. Rockwell, Flow sturcture associated with multiple jets from a generic catheter tip, *Experiments in Fluids,* 42 (2007) 513-530.

[3] A.W. Chen and E. M. Sparrow, Turbulence modeling for flow in a distribution manifold*, International Journal of Heat and Mass Transfer,* 52 (2009) 1573-1581.

[4] A.W. Chen and E. M. Sparrow, Effect of exit-port geome-try on the performance of a flow distribution manifold, *International Journal of Applied Thermal Engineering*, 29 (2009) 2689-2692.

[5] K. El. Moueddeb, S. F. Barrington and N. Barthakur, Perforated ventilation ducts: Part 1. A model for air flow distribution, *Journal of Agricultural Engineering Research,* 68 (1997) 21-27.

[6] K. El. Moueddeb, S. F. Barrington and N. Barthakur, Perforated ventilation ducts: Part 2. Validation of an air distribution model, *Journal of Agricultural Engineering Research*, 68 (1997) 29-37.

[7] R. K. Singh and R. A. Rao, Simplified theory for flow pattern prediction in perforated tubes, *Nuclear engineering and Design*, 239 (2009) 1725-1732.

[8] F. Payri, A. J. Torregrosa and A. Broatch, Pressure loss characterisation of perforated ducts, *SAE paper* 98028 (1998).

[9] D. W. Zhou and S. J. Lee, Forced convective heat transfer with impinging rectangular jets*, International Journal of heat and mass transfer,* 50 (2007) 1916-1926.

[10] H. Y. Ye, D. H. Kim, K. S. Lee and W. H. Cha, Flow distribution in manifold using modified equal pressure method, *Trans. of KSME(B)* (2008) 2280-2285.

[11] F. Lu, Y. H. Luo and S. M. Yang, Analytical and experimental investigation of flow distribution in manifolds for heat exchangers, *Journal of Hydrodynamics*, 20 (2) (2008) 179-185.

[12] R. L. Plgford, M. Ashraf and Y. D. Mlron, Flow distribution in piping manifolds*, Ind.Eng, Chem. Fundam*, 22 (1983) 463-471.

[13] I. Ieronymidis, D. R. H. Gillespie and P. T. Ireland, Experimental and computational flow field studies of an integrally cast cooling manifold with and without rotation, *ASME turbo Exp 2006*:Power for land, sea and air in Spain (2006) 1041-1053.

[14] R. A. Bajura and E. H. Jones, Flow distribution mani-folds, *Transactions of the ASME*, 76 (1976) 654-666.

[15] M. Kelkar, A. Radmehr, P. J. Kelly and S. V. Patankar, Use of flow network modeling(FNM) for enhancing the design process of electronic cooling systems, *Proceeding International systems packaging symposium*, San Diego, January (1999) 58-63.

[16] S. Mokhtari, V. V. Kudriavtsev and M. Danna, Flow uniformity and pressure variation in multi-outlet flow distribution pipes, *The 1997 ASME pressure vessels and piping conference* (1997) 27-31.

[17] C. L. Liu, H. R. Zhu, J. T. Bai and D. C. Xu, Experimental research on the thermal performance of converging slot holes with different divergence angles, *Experimental thermal and fluid science*, 33 (2009) 808-817.

[18] KS D 3568, Carbon steel square pipes for general structural purposes., *KIS* (2009).

Jeekeun Lee received his Ph. D in fluid engineering from Chonbuk National University, in 1998. He is currently an Associate professor in Department of Mechanical System Engineering, Chonbuk National University, Korea. Prof. Lee's research interests include fuel-injection system etc.